

Axialvector diquark Mass and quark-diquark potential in Σ_c

Soya Nishioka^{a,*} and Noriyoshi Ishii^a

^aRCNP, Osaka university,

1-11, Osaka Ibaraki Mihogaoka, Japan

E-mail: nishioka@rcnp.osaka-u.ac.jp, ishiin@rcnp.osaka-u.ac.jp

The axialvector diquark is studied by using 2+1 flavor Lattice QCD. Being a two-quark object, diquark has a non-neutral color charge. Hence the two-point correlators of diquark fields do not have a particle pole due to the color confinement of QCD, and it is not straightforward to study the diquark mass by lattice QCD by using an exponential fit of a temporal two-point correlator. In order to avoid this difficulty, our strategy is to regard the diquark mass as a mass parameter of an effective quark-diquark model which is constructed by using an extended HAL QCD method based on equal-time quark-diquark Nambu-Bethe-Salpeter (NBS) wave functions. We attempt to calculate the axial-vector diquark mass and the quark-diquark potentials between a charm quark and an axial-vector diquark in the Σ_c baryon. Lattice QCD Monte Carlo calculation is performed by using the 2+1 flavor QCD gauge configurations generated on $32^3 \times 64$ lattice by PACS-CS Collaboration which corresponds to the pion mass of about 700 MeV. As a result, a quark-diquark central potential of Cornell-type and a short-ranged spin-dependent potential are obtained. However, from a quantitative point of view, the ground state convergence of the NBS wave functions are not sufficient so that we obtain a larger string tension and a smaller axial-vector diquark mass than we have expected phenomenologically.

The 41st International Symposium on Lattice Field Theory (LATTICE2024)

28 July - 3 August 2024

Liverpool, UK

*Speaker

1. Introduction

The singly charmed baryons, Λ_c and Σ_c^+ , consist of one up quark, one down quark and one charm quark in the quark model picture. They have different iso-spin quantum numbers: Λ_c is an iso-scalar whereas Σ_c is an iso-vector. This difference arises from the distinct quantum numbers of the ud clusters in Λ_c and Σ_c . The quantum numbers of the ud cluster in Λ_c are $J^P = 0^+$, $I = 0$ and color $\bar{\mathbf{3}}$, while those in Σ_c are $J^P = 1^+$, $I = 1$ and color $\bar{\mathbf{3}}$. The ud cluster in Λ_c is referred to as the scalar (good) diquark, while that in Σ_c is called the axial-vector (bad) diquark. The mass difference between Λ_c and Σ_c , i.e. $m_{\Lambda_c} < m_{\Sigma_c}$, can be attributed to the mass difference of these ud clusters. In fact, the scalar diquark is expected to be lighter than the axial-vector diquark, as suggested by the color-magnetic interaction and the instanton-induced interaction in the quark model, which favor the scalar diquark.

Importance of diquarks extends beyond this charmed baryon example. Diquarks are believed to play significant roles in various QCD phenomena [1]. However, studying diquark properties experimentally is challenging due to QCD color confinement. As a result, most known diquark properties remain qualitative and involve uncontrollable uncertainties, since they are inferred not from direct experiments but from phenomenological arguments based on effective models. One may wonder whether lattice QCD, as a first-principle approach, can provide an alternative means to study the diquarks. However, the standard lattice QCD methods cannot directly probe diquarks due to color confinement. Because two-point correlators lack a particle pole in momentum space, it is impossible to extract a diquark mass using the conventional exponential fit to temporal two-point correlators.

Many efforts have been made to study diquark masses in lattice QCD, with notable works classified into two main approaches: (i) Refs. [2–4] and (ii) Refs. [5–8]. In approach (i), Landau gauge fixing is employed to compute the diquark two-point correlators, after which the standard hadron mass extraction method is applied to these gauge-fixed correlators. While their results align with naive expectations based on phenomenological arguments, further discussion is needed regarding their consistency with color confinement. In approach (ii), a static quark is introduced to neutralize the diquark color charge, and the energy of the total system is measured as the diquark mass. However, the interaction energy between the diquark and the static quark remains unsubtracted, leading to an uncertainty of $O(\Lambda_{\text{QCD}})$.

Recently, another method is proposed in Ref. [9], where, to avoid the difficulty related to the color confinement, the scalar diquark mass is computed as a mass parameter of the quark-diquark model which is constructed by an extension of the HAL QCD potential method [10, 11].

The aim of our study is to investigate the axial-vector diquark using a similar method. Specifically, by applying an extended HAL QCD potential approach to describe the Σ_c baryon as a bound state of a charm quark and an axial-vector diquark, we aim to determine both the axial-vector diquark mass and the quark-diquark potential.

2. Formalism

We begin by recalling that, since the axial-vector diquark has the non-neutral color charge ($\bar{\mathbf{3}}$), two-point correlators of diquark fields do not possess a particle-pole in the momentum space

due to the color confinement of QCD, which makes it impossible to use a single-exponential fit in order to extract the diquark mass from the temporal two-point correlators. (See Sec. 60.6.3 in Ref. [12].) We would like to avoid this problem in order to obtain the diquark mass from the lattice QCD. Our strategy is to regard the diquark mass as a mass parameter of an effective quark-diquark model which is constructed by HAL QCD potential method by using the equal-time quark-diquark Nambu-Bethe-Salpeter (NBS) wave functions generated by lattice QCD.

To follow the strategy, we consider the equal-time quark-diquark NBS wave function for Σ_c^{++} in the center of mass frame in Rarita-Schwinger form in the Coulomb gauge as

$$\psi_{i\alpha}(\vec{x} - \vec{y}; J, M) \equiv \langle 0 | D_{ai}(\vec{x}) q_{a\alpha}(\vec{y}) | \Sigma_c^{++}(J, M) \rangle, \quad (1)$$

where $|0\rangle$ denotes the QCD vacuum and $| \Sigma_c^{++}(J, M) \rangle$ denotes the ground state for the even parity Σ_c^{++} baryon in the rest frame with J and M being the total angular momentum and the magnetic quantum number. In this paper, we restrict ourselves to the case with $J = 1/2$ and $3/2$. $q_{a\alpha}(y)$ denotes the Dirac spinor field for the charm quark with the color index $a = 1, 2, 3$ and the Dirac index $\alpha = 1, 2$ which is restricted to the upper components in the Dirac non-relativistic representation. $D_{ai}(x)$ denotes the composite axial-vector diquark field with $i = 1, 2, 3$ being the Lorentz index restricted to the spatial subspace, which is defined as

$$D_{ai}(x) \equiv \epsilon_{abc} u_b^T(x) C \gamma_i u_c(x), \quad (2)$$

where $u(x)$ denotes the u quark field and $C \equiv \gamma_4 \gamma_2$ denotes the charge conjugation matrix.

The equal-time NBS wave functions are related to the quark-diquark four-point correlator in the positive t region as

$$\begin{aligned} C_{i\alpha}(\vec{x}, \vec{y}, t; \mathcal{J}) &\equiv \langle 0 | T [D_{ai}(\vec{x}, t) q_{a\alpha}(\vec{y}, t) \cdot \mathcal{J}(t=0)] | 0 \rangle \\ &= \sum_n \langle 0 | D_{ai}(\vec{x}) q_{a\alpha}(\vec{y}) | n \rangle \cdot e^{-E_n t} \langle n | \mathcal{J} | 0 \rangle, \end{aligned} \quad (3)$$

where $|n\rangle$ denotes the n -th eigenstate of the Hamiltonian and E_n denotes the eigenenergy. \mathcal{J} denotes the source operator. In this paper, we restrict ourselves to the wall source operators defined by

$$\mathcal{J}_{J,M} \equiv \sum_{\vec{x}, \vec{y}, \vec{z}} \bar{q}_{a\alpha}(\vec{x}) \cdot \epsilon_{abc} \bar{u}_b(\vec{y}) C \gamma_i \bar{u}_c^T(\vec{z}) \cdot (1, i; 1/2, \alpha | J, M), \quad (4)$$

where the last factor in the r.h.s. denotes the Clebsch-Gordan coefficients ($j_1 = 1, m_1 = i; j_2 = 1/2, m_2 = \alpha | J, M$) associated with the decomposition $\mathbf{1} \otimes \mathbf{1/2} = \mathbf{1/2} \oplus \mathbf{3/2}$. Hence, in the large t limit, the ground-state NBS wave functions for Σ_c baryon in the spin J channels are obtained as

$$\psi_{i\alpha}(\vec{r} \equiv \vec{x} - \vec{y}; J, M) \propto C_{i\alpha}(\vec{x}, \vec{y}, t; \mathcal{J}_{J,M}). \quad (5)$$

We demand that the quark-diquark NBS wave function satisfy the Schrödinger equation as

$$(\hat{H}_0 + \hat{V}) \psi(\vec{r}; J, M) = (M_J - m_q - m_D) \psi(\vec{r}; J, M), \quad (6)$$

where $\hat{H}_0 \equiv -\nabla^2/(2\mu)$ denotes the kinetic operator with $\mu \equiv \frac{1}{1/m_q + 1/m_D}$ being the reduced mass. m_q and m_D denote the charm quark mass and the axial-vector diquark mass, respectively. For the

time being, we proceed our argument treating m_q and m_D as unknown parameters, which will be determined later. Note that $\mathcal{E}_J \equiv M_J - m_q - m_D$ denotes the ‘‘binding energy’’ of this system with M_J being the mass of the ground state Σ_c^{++} baryon of total angular momentum J . \hat{V} denotes the quark-diquark potential, which is truncated as

$$\hat{V} \simeq V_0(\vec{r}) + V_s(\vec{r}) \mathbf{s}_q \cdot \mathbf{s}_D + \cdots, \quad (7)$$

where $V_0(\vec{r})$ and $V_s(\vec{r})$ denote the central and the spin-dependent potential, respectively, with \mathbf{s}_q and \mathbf{s}_D being the spin operators for the charm quark and the axial-vector diquark, respectively. By using $\mathbf{s}_D \cdot \mathbf{s}_q = -1$ for $J = 1/2$ and $\mathbf{s}_D \cdot \mathbf{s}_q = +1/2$ for $J = 3/2$, the Schrödinger equation Eq. (6) splits into $J = 1/2$ and $3/2$ channels as

$$\begin{aligned} (\hat{H}_0 + V_0(\vec{r}) - V_s(\vec{r})) \psi_{1/2}(\vec{r}) &= (M_{1/2} - m_q - m_D) \psi_{1/2}(\vec{r}) \\ (\hat{H}_0 + V_0(\vec{r}) + (1/2)V_s(\vec{r})) \psi_{3/2}(\vec{r}) &= (M_{3/2} - m_q - m_D) \psi_{3/2}(\vec{r}), \end{aligned} \quad (8)$$

where we introduce a short-hand notation $\psi_J(\vec{r}) \equiv \psi_{i\alpha}(\vec{r}; J, M)$ for notational simplicity. These equations are solved for $V_0(\vec{r})$ and $V_s(\vec{r})$ as

$$\begin{aligned} V_0(\vec{r}) &= \frac{1}{3} (2M_{3/2} + M_{1/2}) - m_q - m_D + \frac{1}{2\mu} \left(\frac{2}{3} \frac{\nabla^2 \psi_{3/2}(\vec{r})}{\psi_{3/2}(\vec{r})} + \frac{1}{3} \frac{\nabla^2 \psi_{1/2}(\vec{r})}{\psi_{1/2}(\vec{r})} \right) \\ V_s(\vec{r}) &= \frac{2}{3} (M_{3/2} - M_{1/2}) - \frac{1}{3\mu} \left(\frac{\nabla^2 \psi_{3/2}(\vec{r})}{\psi_{3/2}(\vec{r})} - \frac{\nabla^2 \psi_{1/2}(\vec{r})}{\psi_{1/2}(\vec{r})} \right). \end{aligned} \quad (9)$$

These relations express $V_0(\vec{r})$ and $V_s(\vec{r})$ by using $\psi_J(\vec{r})$, M_J , m_q and m_D as inputs, where we note that m_q and m_D are treated as unknown mass parameters which should not be determined by the standard method of the exponential fit.

Kawanai and Sasaki encountered the similar problem in $c\bar{c}$ sector, where they proposed a prescription to determine the charm quark mass in a self-consistent manner with HAL QCD method [13]. In their approach, they require that the spin-dependent potential should vanish at long distance. Following their prescription, we impose the condition as

$$V_s(\vec{r}) \rightarrow 0 \quad \text{as} \quad r \rightarrow \infty, \quad (10)$$

which leads us to

$$\mu = - \lim_{r \rightarrow \infty} F_{\text{KS}}(\vec{r}) \quad (11)$$

where we introduce Kawanai-Sasaki function $F_{\text{KS}}(\vec{r})$ for later convenience as

$$F_{\text{KS}}(\vec{r}) \equiv \frac{1}{2(M_{3/2} - M_{1/2})} \left(\frac{\nabla^2 \psi_{3/2}(\vec{r})}{\psi_{3/2}(\vec{r})} - \frac{\nabla^2 \psi_{1/2}(\vec{r})}{\psi_{1/2}(\vec{r})} \right). \quad (12)$$

The reduced mass μ in Eq. (11) together with the charm quark mass m_q obtained by using the Kawanai-Sasaki prescription in the $c\bar{c}$ sector, the axial-vector diquark mass is obtained as

$$m_D = \frac{1}{1/\mu - 1/m_c}. \quad (13)$$

3. Numerical results

3.1 Lattice QCD setup

We employ the 2+1 flavor QCD gauge configurations on $32^3 \times 64$ lattice generated by PACS-CS Collaboration [14]. These gauge configurations are generated by employing the RG improved Iwasaki gauge action at $\beta = 1.90$ and the non-perturbatively $O(a)$ -improved Wilson quark (clover) action at $\kappa_{\text{ud}} = 0.13700$ and $\kappa_s = 0.13640$ with $C_{\text{SW}} = 1.715$. This parameter set corresponds to the lattice spacing $a = 0.0907(13)$ fm ($a^{-1} = 2176(31)$ MeV), the spatial extent $L = 32a \simeq 2.90$ fm. The charm quark is introduced by the quenched approximation by employing the relativistic heavy quark (RHQ) action, for which we use the parameters given in Ref. [15]. Two-point and four-point correlators are calculated by using the quark propagators which are obtained with the wall source after the Coulomb gauge fixing is applied to the gauge configurations. Statistics is improved by using 64 source points by temporally shifting the gauge configurations. The time-reversal and the charge conjugation symmetries are also used to double the statistics. Statistical errors are estimated with the Jackknife prescription employing the bin size of 20 configurations. Some reference hadron masses obtained by this setup are given as follows: $m_N \simeq 1583$ MeV, $m_\pi \simeq 702$ MeV, $m_{\eta_c} \simeq 3025$ MeV, $m_{J/\psi} \simeq 3144$ MeV, $m_{\Lambda_c^{1/2+}} \simeq 2690$ MeV, $m_{\Sigma_c^{1/2+}} \simeq 2777$ MeV and $m_{\Sigma_c^{3/2+}} \simeq 2859$ MeV.

3.2 Results

The results of four-point correlators are shown in Figure 1, where the normalized four-point correlator $\tilde{C}(\vec{r}, t) \equiv C(\vec{r}, t)/C(\vec{0}, t)$ is plotted against r for $t/a = 6, 10, 14, 18, 22$. We see that the convergence is quicker in the short distance region, while it is slower in the long distance region. If we restrict ourselves to the spatial region $r/a \lesssim 7$, rough convergence is achieved at $t/a = 18$. (For $r/a \gtrsim 7$, the convergence becomes gradually worse and the error bar becomes larger.) In what follows, we accept the 4-point correlators at $t/a = 18$ as roughly converged NBS wave functions, and proceed our calculations.

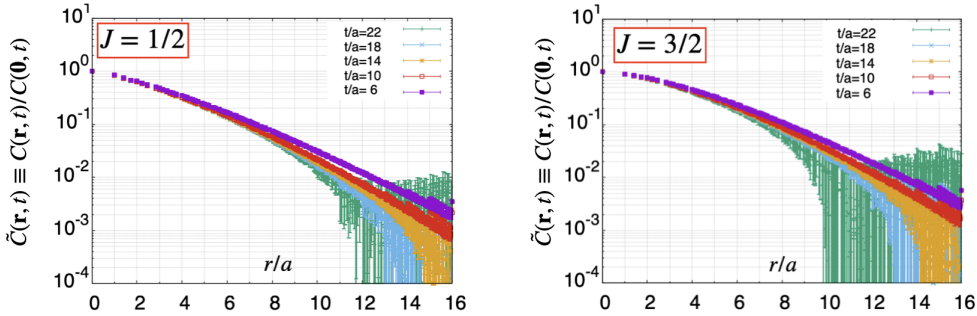


Figure 1: Normalized four-point correlators $\tilde{C}(\vec{r}, t) \equiv C(\vec{r}, t)/C(\vec{0}, t)$ for $J = 1/2$ (left) and $J = 3/2$ (right).

Figure 2 shows the plot of Kawanai-Sasaki function $F_{\text{KS}}(r)$ against r for $t/a = 18$. The purple curve denotes the result of the 2-Gaussian fit employing the functional form: $f(r) \equiv A \exp(-Br^2) + C \exp(-Dr^2) + E$, where A, B, C, D and E are used as fit parameters. Since the long distance limit of $F_{\text{KS}}(r)$ is obtained from the constant part of the fit function, we obtain the reduced mass: $\mu = -\lim_{r \rightarrow \infty} F_{\text{KS}}(r) = -E \simeq 600$ MeV. By applying the Kawanai-Sasaki prescription to

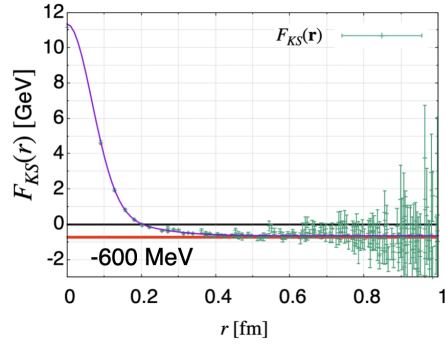


Figure 2: Kawanai Sasaki function $F_{KS}(r)$ for $t/a = 18$.

the $c\bar{c}$ sector, we obtain the charm quark mass $m_q \simeq 1950$ MeV. By using Eq. (13), we obtain the axial-vector diquark mass $m_D \simeq 867$ MeV, which is significantly smaller than the scalar diquark mass $m_{SD} \simeq 1273$ MeV obtained in Ref. [9], where the same gauge configurations with the same pion mass are employed. The main reasons for this underestimate seem to be the following two: (i) ground-state convergence of the four-point correlators are not sufficient at long distance, which results in an uncertainty in the evaluation of the constant part of $F_{KS}(r)$. (ii) Ambiguity in the charm quark mass. In Ref. [9], significantly smaller charm quark mass $m_q \simeq 1686$ MeV is used than our charm quark mass $m_q \simeq 1950$ MeV. One reason for this discrepancy is that Ref. [9] uses the odd parity $c\bar{c}$ spectrum to determine the charm quark mass instead of Kawanai-Sasaki prescription. Another reason is that fit of this $c\bar{c}$ central potential is technically involved. In order to perform a quantitative fit in the whole spatial region, the simple Cornell-type functional form is not enough, and at least $\log(r)$ term has to be included [9]. In addition, at short distance, the violation of the rotational symmetry is severe.

Figure 3 shows the quark-diquark potentials obtained from Eq. (9) with $m_q \simeq 1950$ MeV and $m_D \simeq 867$ MeV. We see that the spin-dependent potential $V_s(r)$ is short ranged and that the quark-diquark central potential $V_0(r)$ is of Cornell-type: $V_{\text{Cornell}}(r) \equiv -A/r + \sigma r + \text{const}$. For comparison, $c\bar{c}$ potential is added in Figure 3. These two central potentials are fitted with $V_{\text{Cornell}}(r)$, which leads to $A \simeq 86$ MeV fm and $\sqrt{\sigma} \simeq 565$ MeV for quark-diquark sector, and $A \simeq 103$ MeV fm and $\sqrt{\sigma} \simeq 459$ MeV for $c\bar{c}$ sector. We see that, at long distance, the quark-diquark central potential is a bit steeper than the $c\bar{c}$ central potential, which may be an artifact caused by the underestimate of the reduced mass μ through the overall factor in Eq. (9).

For quantitative calculation of the axial-vector diquark mass, the most important thing is to improve the ground-state convergence of the quark-diquark four-point correlator. For this purpose, we plan to use the time-dependent HAL QCD method [16] and the variational method to improve the source operators in the near future.

4. Conclusion

We have studied the axial-vector diquark mass and the quark-diquark potentials between an axial-vector diquark and a charm quark by using 2+1 flavor lattice QCD.

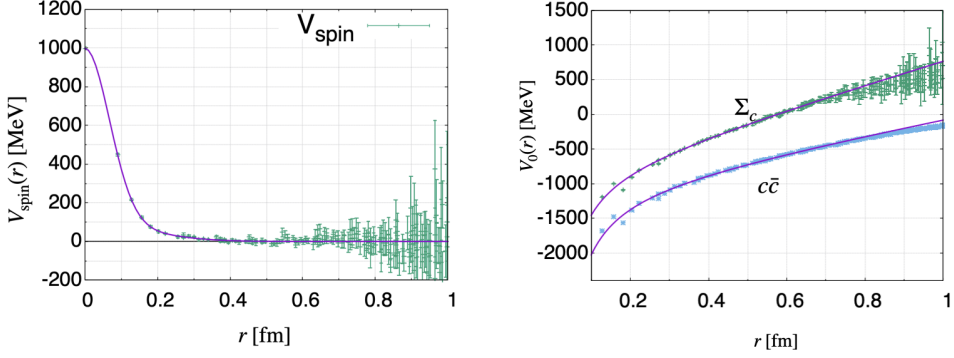


Figure 3: The spin dependent quark-diquark potential $V_s(r)$ (left) and the central quark-diquark potential $V_0(r)$ together with the central $c\bar{c}$ potential (right).

Since the axial-vector diquark has non-neutral color charge ($\bar{\mathbf{3}}$), the two-point correlator does not have a particle-pole in the momentum space due to the color confinement of QCD, so that the standard method to calculate the hadron mass by an exponential fit of the temporal two-point correlator is not usable to obtain the diquark mass. In this paper, to avoid this difficulty, we have resorted to the Kawanai-Sasaki extension of the HAL QCD potential method, where the diquark mass and quark-diquark potentials are obtained simultaneously by demanding that the spin-dependent quark-diquark potential should vanish in the long distance limit.

Numerical calculations have been performed by using the 2+1 flavor QCD gauge configurations generated on $32^3 \times 64$ lattice by PACS-CS Collaboration employing the RG-improved Iwasaki gauge action at $\beta = 1.90$ and the non-perturbatively $O(a)$ -improved Wilson quark (clover) action at $\kappa_{\text{ud}} = 1.3700$ and $\kappa_s = 1.3640$ with $C_{\text{SW}} = 1.715$. The charm quark has been incorporated with the quenched approximation by using the relativistic heavy quark (RHQ) action. The setup lead to the lattice spacing $a^{-1} = 2176(31)$ MeV ($a = 0.0907(13)$ fm) and the pion mass $m_\pi \simeq 702$ MeV.

By using the charm quark mass $m_q \simeq 1950$ MeV which was obtained by applying the Kawanai-Sasaki extension of the HAL QCD method to the $c\bar{c}$ sector, we have obtained the axial-vector diquark mass $m_D \simeq 867$ MeV, which is significantly smaller than the scalar diquark mass $m_{SD} \simeq 1273$ MeV obtained by a similar method with exactly the same gauge configurations in Ref. [9]. The underestimate of the axial-vector diquark mass has seemed to be mainly due to the insufficient ground-state convergence of the quark-diquark four-point correlators in the long spatial distance region.

We have also obtained the quark-diquark potentials between an axial-vector diquark and a charm quark. We have obtained the spin-dependent potential $V_s(r)$ which is of short-ranged and the central potential $V_0(r)$ which is of Cornell-type. However, we have seen that the long distance behavior of $V_0(r)$ is steeper than that of the central $c\bar{c}$ potential, which has seemed to be due to the underestimate of the axial-vector diquark mass.

In the future, we will try to improve the ground-state convergence of the quark-diquark four-point correlators by using the time-dependent HAL QCD method. We will also try to improve the source operators by using the variational method. These improvements are important in making

a precise comparison of the axial-vector diquark and the scalar diquark. We are interested in the quark mass dependence of our results, because the calculations in this paper have been carried out by employing the gauge configurations which correspond to rather heavy pion mass.

Acknowledgments

Lattice QCD calculations have been done by using the supercomputer SQUID at the Cyber Media Center (CMC) of Osaka University under the support of Research Center for Nuclear Physics (RCNP) of Osaka University. We thank PACS-CS Collaboration and JLDG/ILDG for the 2+1 flavor QCD gauge configurations. We also thank the lattice QCD library bridge++ [17], a modified version of which is used for our calculation. This work was supported by JST SPRING, Grant Number JPMJSP2138 and JSPS KAKENHI Grant Number JP21K03535.

References

- [1] R. L. Jaffe. Exotica. *Nucl. Phys. B Proc. Suppl.*, 142:343–355, 2005.
- [2] M. Hess, F. Karsch, E. Laermann, and I. Wetzorke. Diquark masses from lattice QCD. *Phys. Rev. D*, 58:111502, 1998.
- [3] Ronald Babich, Nicolas Garron, Christian Hoelbling, Joseph Howard, Laurent Lellouch, and Claudio Rebbi. Diquark correlations in baryons on the lattice with overlap quarks. *Phys. Rev. D*, 76:074021, 2007.
- [4] Yujiang Bi, Hao Cai, Ying Chen, Ming Gong, Zhaofeng Liu, Hao-Xue Qiao, and Yi-Bo Yang. Diquark mass differences from unquenched lattice QCD. *Chin. Phys. C*, 40(7):073106, 2016.
- [5] C. Alexandrou, Ph. de Forcrand, and B. Lucini. Evidence for diquarks in lattice QCD. *Phys. Rev. Lett.*, 97:222002, 2006.
- [6] Konstantinos Orginos. Diquark properties from lattice QCD. *PoS*, LAT2005:054, 2006.
- [7] Jeremy Green, John Negele, Michael Engelhardt, and Patrick Varilly. Spatial diquark correlations in a hadron. *PoS*, LATTICE2010:140, 2010.
- [8] Anthony Francis, Philippe de Forcrand, Randy Lewis, and Kim Maltman. Diquark properties from full QCD lattice simulations. *JHEP*, 05:062, 2022.
- [9] Kai Watanabe. Quark-diquark potential and diquark mass from lattice QCD. *Phys. Rev. D*, 105(7):074510, 2022.
- [10] Noriyoshi Ishii, Sinya Aoki, and Tetsuo Hatsuda. Nuclear force from lattice qcd. *Physical review letters*, 99(2):022001, 2007.
- [11] Sinya Aoki, Tetsuo Hatsuda, and Noriyoshi Ishii. Theoretical foundation of the nuclear force in qcd and its applications to central and tensor forces in quenched lattice qcd simulations. *Progress of theoretical physics*, 123(1):89–128, 2010.
- [12] R. L. Workman et al. Review of Particle Physics. *PTEP*, 2022:083C01, 2022.
- [13] Taichi Kawanai and Shoichi Sasaki. Interquark potential with finite quark mass from lattice QCD. *Phys. Rev. Lett.*, 107:091601, 2011.
- [14] S. Aoki et al. 2+1 Flavor Lattice QCD toward the Physical Point. *Phys. Rev. D*, 79:034503, 2009.
- [15] Y. Namekawa et al. Charm quark system at the physical point of 2+1 flavor lattice QCD. *Phys. Rev. D*, 84:074505, 2011.
- [16] Noriyoshi Ishii, Sinya Aoki, Takumi Doi, Tetsuo Hatsuda, Yoichi Ikeda, Takashi Inoue, Keiko Murano, Hidekatsu Nemura, and Kenji Sasaki. Hadron–hadron interactions from imaginary-time Nambu–Bethe–Salpeter wave function on the lattice. *Phys. Lett. B*, 712:437–441, 2012.

- [17] S. Ueda, S. Aoki, T. Aoyama, K. Kanaya, H. Matsufuru, S. Motoki, Y. Namekawa, H. Nemura, Y. Taniguchi, and N. Ukita. Development of an object oriented lattice QCD code 'Bridge++'. *J. Phys. Conf. Ser.*, 523:012046, 2014.